

Effective Temperature of Red Blood Cell Membrane Fluctuations

Eyal Ben-Isaac¹, YongKeun Park², Gabriel Popescu³, Frank L.H. Brown⁴, Nir S. Gov^{*1} and Yair Shokef^{†5}

¹ *Department of Chemical Physics, The Weizmann Institute of Science, Rehovot 76100, Israel*

² *Department of Physics, Korea Advanced Institute of Science and Technology, Daejeon 305-701, Republic of Korea*

³ *Quantitative Light Imaging Laboratory, Department of Electrical and Computer Engineering, Beckman Institute for Advanced Science & Technology,*

University of Illinois at Urbana-Champaign, Urbana, IL 61801, USA

⁴ *Department of Chemistry and Biochemistry and Department of Physics,*

University of California Santa Barbara, CA 93106, USA

⁵ *Department of Materials and Interfaces, The Weizmann Institute of Science, Rehovot 76100, Israel*

Biologically driven non-equilibrium fluctuations are often characterized by their non-Gaussianity or by an “effective temperature”, which is frequency dependent and higher than the ambient temperature. We address these two measures theoretically by examining a randomly kicked “particle”, with a variable number of kicking “motors”. We show how these two indicators of non-equilibrium behavior can contradict. We compare our results with new experiments on shape fluctuations of red-blood cell membranes, for which these two indicators were independently measured.

PACS numbers: 87.10.Mn, 87.16.D-, 87.16.Ln, 05.40.-a

Recent experimental and theoretical studies of biological systems have confronted the issue of active elements which give rise to motion that distinguishes living matter from inanimate soft-matter systems. Examples range from molecular motors in the cytoskeleton [1] and active membrane pumps [2] to larger scale objects such as swimming bacteria [3]. The study of these biological systems shares similarities with other non-equilibrium systems such as driven granular matter. In both cases it is unclear how to define useful measures for non-equilibrium “activity”. Spontaneous fluctuations may be compared with the response of the system to small external perturbations, to define an effective temperature T_{eff} using the fluctuation-dissipation formalism [4]. In most cases T_{eff} is frequency dependent (unlike the thermal case), and is larger than the ambient temperature. These features quantify the activity in the system at hand and distinguish it from the thermal case. Another parameter that is useful for characterizing deviations from equilibrium is the kurtosis κ of the distribution function; deviations of the kurtosis from its Gaussian value ($\kappa_G = 3$) indicate that the system is not in equilibrium [5–7].

In this Letter we address the question of how the two measures described above, T_{eff} and κ , correlate (or not) with each other, and which properties of the non-equilibrium system do they describe. We focus on red-blood cells (RBC) and present new experimental measurements, but obtain results on the non-equilibrium statistical mechanics of active systems in general. We introduce a simple model of a randomly kicked “particle”, with a variable number of kicking “motors” (force producing elements). Our generalized particle and motors

may represent different objects in different systems, and we will be more specific when comparing to experiments. We compute both T_{eff} and κ , and demonstrate that there can be conditions where these two non-equilibrium indicators contradict. Unlike recent studies [8] we explicitly explore the effect of the number of active motors, and show that for multiple motors the velocity fluctuations may be close to Gaussian whereas far from equilibrium T_{eff} always has a strong frequency dependence.

Model. We consider the following overdamped Langevin equation for the velocity v ,

$$\dot{v} = -\lambda v + f_T + f_A + f_R. \quad (1)$$

λ is the damping coefficient. The thermal force $f_T(t)$ is an uncorrelated Gaussian white noise: $\langle f_T(t)f_T(t') \rangle = 2\lambda T_B \delta(t - t')$, with T_B the ambient temperature, and Boltzmann’s constant set to $k_B = 1$. For the active force $f_A(t)$ we assume that each of the N_m “motors” produces pulses of force $\pm f_0$, of duration $\Delta\tau$. While the pulses turn on randomly as a Poisson process with an average waiting time τ , unless otherwise stated, we take a constant pulse length $\Delta\tau$. The power stroke of molecular motors is a realization for such a relatively well defined impulse length [9]. We also consider stochastic pulse lengths with an arbitrary distribution $P(\Delta\tau)$, and show that if $P(\Delta\tau)$ is Poissonian, the force correlations reduce to the shot-noise form studied in [10]. f_R is a small force applied on the system to probe its linear response.

Due to the linearity of Eq. (1), its solution is the following superposition $v(t) = v_T(t) + v_A(t) + v_R(t)$ of the solutions $v_T(t)$, $v_A(t)$, and $v_R(t)$ to the equations

$$\dot{v}_T = -\lambda v_T + f_T, \dot{v}_A = -\lambda v_A + f_A, \dot{v}_R = -\lambda v_R + f_R. \quad (2)$$

To measure the response we apply $f_R = F_0 e^{i\omega t}$ and find $\langle \delta x(t) \rangle = \chi_{xx}(\omega) F_0 e^{i\omega t}$, with $\chi_{xx}(\omega) = (\omega(i\lambda - \omega))^{-1}$, irrespective of the active force [11].

*nir.gov@weizmann.ac.il

†yair.shokef@weizmann.ac.il

We measure correlations when $f_R = 0$, thus $v_R = 0$. f_T and f_A are uncorrelated, hence so are v_T and v_A :

$$S_{vv}(\omega) \equiv \int_{-\infty}^{\infty} e^{-i\omega t} \langle v(t)v(0) \rangle dt = S_T(\omega) + S_A(\omega) \quad (3)$$

where $S_\alpha(\omega) \equiv \int_{-\infty}^{\infty} e^{-i\omega t} \langle v_\alpha(t)v_\alpha(0) \rangle dt$ ($\alpha = A, T$). The thermal component $f_T(t)$ is white, thus, from Eq. (2), $\langle v_T(t)v_T(0) \rangle = \langle v_T^2 \rangle e^{-\lambda t}$, and $S_T(\omega) = 2\lambda \langle v_T^2 \rangle / (\lambda^2 + \omega^2)$. The active component $f_A(t)$ is a sum over pulses, $f_A(t) = \sum_i \sigma_i f_p(t - t_i)$, with $\sigma_i = \pm 1$ the sign of pulse i , t_i the time at which it started, and $f_p(t)$ contains the time dependence of the force in a given pulse. By the linearity of Eq. (2), $v_A(t) = \sum_i \sigma_i v_p(t - t_i)$, with $v_p(t)$ the velocity change following a single pulse. The signs of the pulses are uncorrelated, $\langle \sigma_i \sigma_j \rangle = \delta_{i,j}$, hence $\langle v_A(t)v_A(0) \rangle = \frac{N_m}{\tau + \Delta\tau} \int_0^\infty v_p(0)v_p(t') dt'$, where the prefactor comes from the average number of pulses per unit time. We define $v_0 \equiv f_0/\lambda$ and eventually have [11]

$$S_A(\omega) = \frac{2N_m v_0^2 \lambda^2 [1 - \cos(\omega \Delta\tau)]}{(\tau + \Delta\tau) \omega^2 (\lambda^2 + \omega^2)}. \quad (4)$$

Effective Temperature. In thermodynamic equilibrium, the fluctuation-dissipation theorem connects the imaginary part of χ_{xx} to the position autocorrelation, $S_{xx}(\omega) \equiv \int_{-\infty}^{\infty} e^{-i\omega t} \langle \delta x(t) \delta x(0) \rangle dt = -\omega^{-2} S_{vv}(\omega)$, by: $\text{Im}[\chi_{xx}(\omega)] = \frac{\omega}{2T} S_{xx}(\omega)$. For non-equilibrium steady states we define a frequency-dependent effective temperature

$$T_{\text{eff}}(\omega) \equiv \frac{\omega S_{xx}(\omega)}{2\text{Im}[\chi_{xx}(\omega)]} = T_B + \frac{N_m v_0^2 \lambda [1 - \cos(\omega \Delta\tau)]}{(\tau + \Delta\tau) \omega^2}. \quad (5)$$

Successive pulses as well as simultaneous activity of multiple motors cause the velocity to have a complicated time dependence. However, due to the randomness in the force direction ($\sigma_i = \pm 1$), cross terms in the correlation function cancel, and the time between pulses enters only through the density of pulses per unit time. Hence the results given above do not depend on the distribution of waiting times between pulses, but only on its average, τ .

Moreover, our results may be extended to a stochastic pulse length [11]. For motors which switch both on and off in Poisson processes, we obtain shot-noise force correlations $\langle f_A(t)f_A(0) \rangle = \langle \Delta\tau \rangle^{-1} \exp(-t/\langle \Delta\tau \rangle)$ and $T_{\text{eff}} = T_B + N_m v_0^2 \lambda (\tau + \langle \Delta\tau \rangle)^{-1} (\omega^2 + \langle \Delta\tau \rangle^{-2})^{-1} / 2$.

Note that alternative definitions of the effective temperature have appeared in the context of granular gases [12]. Unlike that system, here we do not identify a non-equilibrium situation where $T_{\text{eff}}(\omega) = \text{const.}$.

Figure 1 shows the excellent agreement of T_{eff} with numerical simulations. In the high-frequency limit the active contribution vanishes and only the background thermal fluctuations contribute, so that $T_{\text{eff}} \rightarrow T_B$. Around $\omega = 1/\Delta\tau$, T_{eff} rises and as $\omega \rightarrow 0$, it approaches a constant value in the limit of small frequencies ($\omega \ll \Delta\tau^{-1}$):

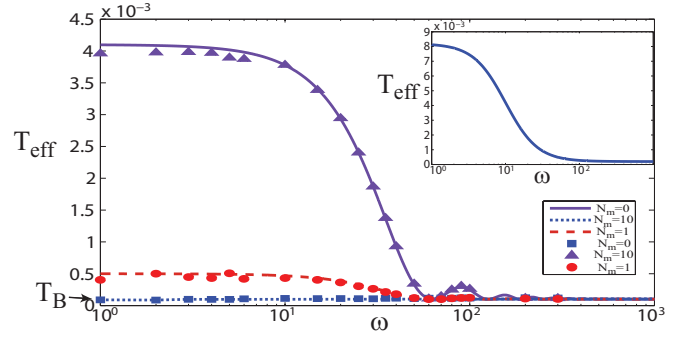


FIG. 1: Effective temperature vs frequency: Numerical simulations (symbols) agree perfectly with the analytic expression (Eq. 5, solid lines), for different numbers N_m of motors (see legend). $\lambda = 50$, $\Delta\tau = 0.1$, $\tau = 0.15$, $T_B = 10^{-4}$, $v_0 = 0.02$. Inset: pulses of random duration with $\langle \Delta\tau \rangle = 0.1$.

$T_{\text{eff}}(0) = T_B + N_m v_0^2 \lambda \Delta\tau^2 / (\tau + \Delta\tau)$. Nevertheless the system does not behave as a thermal bath at an elevated temperature, since the velocity distribution is non-Gaussian (see below). We see that $T_{\text{eff}} - T_B$ increases linearly with the number of motors, and approaches 0 in the limit $\lambda \Delta\tau \rightarrow 0$. The inset shows how the variability in pulse length affects not only the frequency dependence of T_{eff} but also its value in the low ω limit.

Velocity Distribution and Kurtosis. In Fig. 2a we plot the velocity distribution function $P(v)$, from the numerical simulation. As expected, the distribution is highly non-Gaussian for a single motor. Interestingly, for small $\lambda \Delta\tau$ and in the presence of multiple motors, $P(v)$ may retain its Gaussian form, even though the system is very far from equilibrium, as can be seen in the strong frequency dependence of $T_{\text{eff}}(\omega)$ in Fig. 1, and in the fact that $\langle v^2 \rangle$ (the reciprocal of the slope in Fig. 2a) is significantly larger than T_B . For our model we can exactly calculate [11]: $\langle v^2 \rangle = T_B + (N_m v_0^2 \lambda (\lambda \Delta\tau + e^{-\lambda \Delta\tau} - 1)) / (\lambda (\tau + \Delta\tau))$. Let us emphasize that $\langle v^2 \rangle \neq T_{\text{eff}}(0)$, but rather in the limit $\lambda \Delta\tau \rightarrow 0$ we find that $\langle v^2 \rangle = 2T_{\text{eff}}(0)$.

A common measure for non-Gaussianity is the kurtosis, $\kappa \equiv \langle v^4 \rangle / \langle v^2 \rangle^2$, which we plot in Fig. 2b as a function of the activity and number of motors. We measure the activity by the probability of a single motor to be on: $p_{\text{on}} \equiv \Delta\tau / (\tau + \Delta\tau)$. In order to compute κ we need to calculate $\langle v^4 \rangle$, and this entails taking into account overlaps between pulses. For multiple motors, we avoid this complication by a simplified model [11]. For a single motor, as long as $\lambda \tau \gg 1$, we may ignore overlaps and assume that by the next time the motor shoots, the active component of the velocity following the previous shot has decayed to zero. Hence we average the fourth moment of the velocity $v_p(t)$ following a single pulse, $\langle v_A^4 \rangle = \langle v_p^4 \rangle / (\tau + \Delta\tau)$. Now, $\langle v_T^4 \rangle = 3T_B^2$, and due to the lack of correlation between v_T and v_A , we have $\langle v^2 \rangle = \langle v_T^2 \rangle + \langle v_A^2 \rangle$ and $\langle v^4 \rangle = \langle v_T^4 \rangle + 6\langle v_A^2 \rangle \langle v_T^2 \rangle + \langle v_A^4 \rangle$. Hence the kurtosis is obtained [11]. This applies for

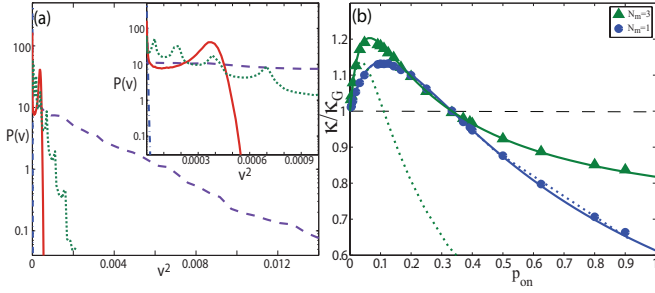


FIG. 2: (a) Velocity distribution function: Thermal case is the dash-dot straight line with slope T_B^{-1} . $N_m = 1$ (solid line), 10 (dashed line). Other parameters as in Fig. 1. Note second peak at v_0 for $N_m = 1$. Dotted line: $N_m = 10$ using $T_B = 10^{-7}$ and $\lambda = 150$. The kurtosis for the active cases are: $\kappa/\kappa_G = 0.85, 0.99, 0.96$, respectively. Inset shows the same figure in the range of small velocities. (b) Kurtosis vs motor activity from numerical simulations (symbols), compared to the analytic expression ignoring pulse overlaps (dotted lines), and to the model of shifted Gaussians (solid lines).

$\lambda\tau \gg 1$, but fails for multiple motors (see Fig. 2b). A simple model which works rather well at all number of motors, approximates the distribution as a sum of shifted thermal Gaussians [11]. As long as $\lambda\Delta\tau \gg 1$, the contribution to the velocity distribution due to the rise and decay before and after each pulse is small, and this approximation gives a very good description (see Fig. 2b).

The most outstanding feature that we find is the non-monotonic dependence of the kurtosis on the motor activity. In fact, the kurtosis can retain its Gaussian value even for a non-equilibrium system ($p_{on} > 0$). For the distributions shown in Fig. 2a the kurtosis is close to $\kappa_G = 3$, except for the single motor, even when the distribution is visibly non-Gaussian (10 motors). At small p_{on} the deviation from Gaussianity increases with the number of motors (Fig. 2b), while as $p_{on} \rightarrow 1$, the distribution approaches a Gaussian with increasing number of motors (manifestation of the central limit theorem). Comparing with T_{eff} we find that both measures of non-equilibrium behavior increase with increasing activity in the $p_{on} \rightarrow 0$ limit, while as $p_{on} \rightarrow 1$ they contradict.

Experiments. The activity of the RBC membrane was recently measured in two different experiments, which found indications for non-equilibrium fluctuations when the chemical energy source of ATP is available. Before comparing with our model we note that the membrane undulations are described by the following over-damped analogue of Eq. (1) [15],

$$\dot{h}_q = -\lambda_q h_q + \mathcal{O}_q [F_T(q, t) + F_A(q, t)] \quad (6)$$

where h_q is the amplitude of the membrane deflection at wavevector q , $\lambda_q = \mathcal{O}_q(\bar{\kappa}q^4 + \sigma q^2)$ is the response of the membrane due to the elastic restoring forces of curvature and tension (with bending modulus $\bar{\kappa}$ and membrane tension σ), $\mathcal{O}_q = (4\eta q)^{-1}$ is the Oseen interaction

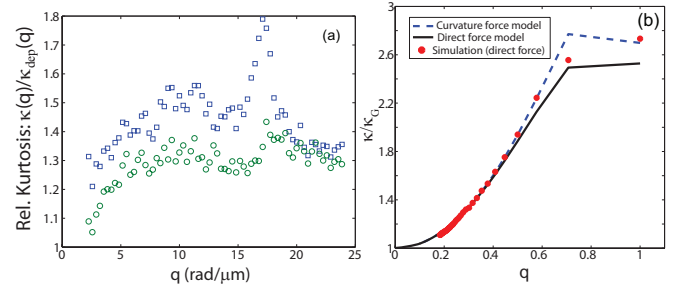


FIG. 3: (a) Relative kurtosis vs wavevector: Squares (circles) are for natural (after 6hrs starvation) RBC. $\kappa_G(q)$ was extracted from the data on ATP-depleted cells, starved for 24hrs. (b) Calculated dependence of κ from our model, mapped to q -space (Eq. 6, using $p_{on} = 0.07$). The dimensionless q is determined in this calculation by varying the number of motors ($N_m = 1, 2, \dots, 30$) and taking: $N_m \propto q^{-2}$.

kernel for a flat membrane in free fluid and η the viscosity of the surrounding fluid. The thermal force satisfies $\langle F_T(q, t) F_T(-q, t') \rangle = 2T_B \mathcal{O}_q^{-1} \delta(t - t')$, and $F_A(q, t)$ is the Fourier transform of the active force. For the active forces we consider two cases; a direct force and a curvature-force [10], both with shot-noise correlations, as we derived above for pulses of random duration.

The first experiment [7] measured the spatial dependence of the membrane fluctuations, and extracted the probability distribution $P(h_q)$, from which the kurtosis was obtained. Here, $\kappa > \kappa_G$ was found for ATP-containing cells. In Fig. 3a we present new data showing that κ increases with q and with the ATP concentration. We measured the dynamic fluctuations in the RBC membrane with the different ATP concentration, from which κ was calculated [11]. Comparing these observations with our model (Fig. 2) we note that the increase in the kurtosis with ATP concentration indicates that the entire observed change is limited to p_{on} close to zero, which means that $\tau \gg \Delta\tau$. We therefore conclude that in this system there is a long recovery time for each motor. This agrees with the proposed mechanism of membrane fluctuations [13], whereby ATP induces the release of membrane-anchored filaments. The release event ($\Delta\tau$) is fast compared to the time it takes the released polymer to find its anchor on the membrane and re-attach (τ).

Next, we compute the q -dependence of the kurtosis using our single-particle model and the similarity between Eqs. (1,6). We map each mode q of the membrane to a single particle as follows; the number of motors that act on the membrane area involved in the motion of mode q is given by: $N_m \propto q^{-2}$ (simply the number of motors in the membrane area of wavelength $2\pi/q$, assuming they are uniformly distributed on the membrane), $F_A \propto q^0, q^2$ (direct and curvature force respectively [10]) and $\langle F_T^2 \rangle \propto q$. The values of the parameters used in this mapping are given in [11]. In Fig. 3b we show that our calculations predict that $\kappa \rightarrow \kappa_G$ as $q \rightarrow 0$, in agreement with the ob-

servations (Fig. 3a), since for the modes of larger wavelength the number of motors increase. The peak in the experimental observations may indicate the wavelength corresponding to a single active unit (“motor”) in the RBC cytoskeleton [7]. Note that using our single-particle calculation for the dynamics of an extended object such as the membrane is only a qualitative approximation.

The second experiment measured the frequency dependence of the height fluctuations at a single point on the cell membrane, and found increased fluctuations at low frequencies ($f < 10\text{Hz}$) compared to cells depleted of ATP. In [14] most of the difference was attributed to the ATP-induced changes in the elastic moduli of the membrane and the cytoskeleton [13], and only a small fraction of ~ 1.2 that remained was denoted as a higher “effective temperature” due to active forces. In Fig. 4 we plot the calculated effective temperature of the system, as defined by the fluctuation-dissipation theorem (5) [11]. We find that the effective temperature approaches the ambient temperature for large frequencies $\omega \gg \tau^{-1}$, and increases for frequencies $\omega \leq \tau^{-1}$. There is even a peak in this measure for the curvature-force model. The values of T_{eff} reach up to 10, and depend on the lateral size of the membrane L ; in the limit of $\omega \rightarrow 0$ we find that $T_{\text{eff,direct}} - T_B \propto q_{\text{min}}^{-1}$ while $T_{\text{eff,curv}} - T_B \propto q_{\text{min}}$, where $q_{\text{min}} = 2\pi/L$ (inset of Fig. 4).

To simplify the analysis, we assumed that the elastic moduli do not change by the ATP, which only enters through the strength of active fluctuations. Not surprisingly the values of T_{eff} that we find are much larger than the factor of ~ 1.2 deduced in the experiment [14]. The only way to decouple the ATP-induced changes to the elastic moduli from the increase in effective temperature is to measure the response in addition to the fluctuations, and this awaits future experiments. Note that for the curvature force, the effective temperature decreases with decreasing ω , and even approaches the equilibrium value at $\omega = 0$ for a large membrane domain ($L \rightarrow \infty$). Another indication for an increase of effective temperature with frequency was found for a driven granular system [16].

By comparing the calculated and observed [14] frequency dependence of T_{eff} and the power spectral density [11], we can estimate the properties of the active “motors” in this system: $\Delta\tau \simeq 100\text{msec}$, $p_{\text{on}}f_0^2 \simeq (\bar{\kappa}/r)^2$, where $r \simeq 100\text{nm}$, $\bar{\kappa} \simeq 90k_B T$, and the motor density $n = 1/r^2$. These parameters agree with the physical interpretation of the active force as arising from “pinching” of the membrane by a cytoskeleton network of spectrin filaments [13].

Conclusion. We have presented a simple model for an active system, for which we can derive two measures to characterize its non-equilibrium nature. These two measures do not always agree. In particular, in the presence of multiple motors, the kurtosis returns to the value of a Gaussian distribution, while the effective temperature may still exhibit strong frequency depen-

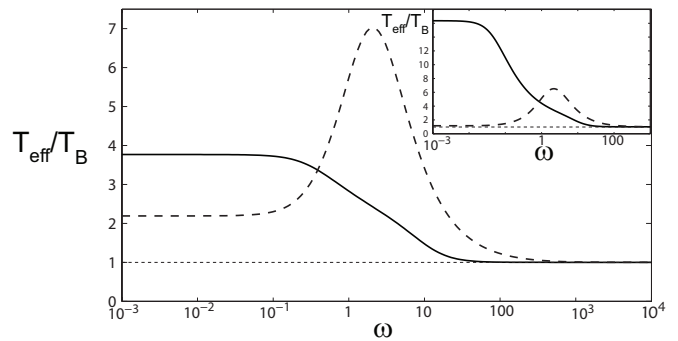


FIG. 4: Effective temperature for a free membrane of lateral size $L = 8\mu\text{m}$, driven by the direct force (solid line) and curvature force (dashed line). Inset: the results for $L = 50\mu\text{m}$.

dence. We showed that Gaussian distributions may arise for active systems even for a small number of motors, while large deviations from Gaussian distributions can be maintained for large number of motors. The effective temperature that we calculated is explicitly dependent on the number of motors (N_m) and their intrinsic properties ($f_0, \tau, \Delta\tau$). Our present analysis gives a detailed and general treatment, for any type of pulse-length distribution.

Finally, we compared the results of our model with recent observations of ATP-driven activity in RBC, and demonstrated how they can give insight to the underlying active mechanism. Future experiments could use the calculated properties to better characterize the nature of the active forces in various cellular membranes. We expect our results to be useful for the analysis of other active systems, both biological [6] and non-biological [17, 18].

Acknowledgments: Y.S. thanks ISF grant 54/08 for support. N.S.G. thanks the Alvin and Gertrude Levine Career Development Chair, BSF grant No. 2006285 and the Harold Perlman Family for their support.

-
- [1] D. Mizuno, C. Tardin, C.F. Schmidt and F.C. MacKintosh, *Science* **315**, 370 (2007); F.C. MacKintosh and C.F. Schmidt, *Current Opinion in Cell Biology* **22**, 29 (2010).
 - [2] M.D. El Alaoui Faris *et al.*, *Phys. Rev. Lett.* **102**, 038102 (2009); P. Girard, J. Prost and P. Bassereau, *Phys. Rev. Lett.* **94**, 088102 (2005).
 - [3] X.-L. Wu and A. Libchaber, *Phys. Rev. Lett.* **84**, 3017 (2000); D.T.N. Chen *et al.*, *Phys. Rev. Lett.* **99**, 148302 (2007); J. Tailleur and M.E. Cates, *EPL* **86**, 60002 (2009).
 - [4] H.B. Callen and T.A. Welton, *Phys. Rev.* **83**, 34 (1951); P.C. Hohenberg and B.I. Shraiman, *Physica D* **37**, 109 (1989); L.F. Cugliandolo, J. Kurchan and L. Peliti, *Phys. Rev. E* **55**, 3898 (1997).
 - [5] I. Goldhirsch and M.-L. Tan, *Phys. Fluids* **8**, 1752 (1996); T.P.C. van Noije and M.H. Ernst, *Gran. Matter* **1**, 57 (1998); D.L. Blair and A. Kudrolli, *Phys. Rev. E* **64**,

- 050301 (2001); **67**, 041301 (2003).
- [6] C.P. Brangwynne, G.H. Koenderink, F.C. MacKintosh and D.A. Weitz, Phys. Rev. Lett. **100**, 118104 (2008).
 - [7] Y. Park *et al.*, PNAS **107**, 1289 (2010).
 - [8] D. Loi, S. Mossa and L.F. Cugliandolo, Phys. Rev. E **77**, 051111 (2008); arXiv:1012.2745; A.J. Levine and F.C. MacKintosh, J. Phys. Chem. B **113**, 3820 (2009); K.I. Morozov and L.M. Pismen, Phys. Rev. E **81**, 061922 (2010).
 - [9] M.J. Tyska and D.M. Warshaw, Cell Motility and the Cytoskeleton **51**, 1 (2002).
 - [10] N. Gov, Phys. Rev. Lett. **93**, 268104 (2004).
 - [11] See EPAPS Document No. [number will be inserted by publisher] for more details on the theory and experiments.
 - [12] Y. Shokef and D. Levine, Phys. Rev. E **74** 051111 (2006); G. Bunin, Y. Shokef and D. Levine, Phys. Rev. E **77** 051301 (2008).
 - [13] N. Gov and S. Safran, Biophys. J. **88**, 1859 (2005); N.S. Gov, Phys. Rev. E **75**, 011921 (2007).
 - [14] T. Betz, M. Lenz, J.-F. Joanny and C. Sykes, PNAS **106**, 15320 (2009).
 - [15] L.C.-L. Lin, N.S. Gov and F.L.H. Brown, J. Chem. Phys. **124**, 074903 (2006).
 - [16] G. D'Anna *et al.*, Nature **424**, 909 (2003).
 - [17] A.R. Abate and D.J. Durian, Phys. Rev. E **72**, 031305 (2005); Phys. Rev. Lett. **101**, 245701 (2008).
 - [18] J. Palacci, C. Cottin-Bizonne, C. Ybert and L. Bocquet, Phys. Rev. Lett. **105**, 088304 (2010).